AGU PUBLICATIONS

JGR

Journal of Geophysical Research: Atmospheres

RESEARCH ARTICLE
10.1002/2016JD025239

Key Points:
- The 20.9/56.9% of collocated MODIS and C-C are identified as clear/cloudy; 9.1/1.8% are clear/cloudy in MODIS but cloudy/clear in C-C
- The 17.7/7.7% of MODIS/C-C observation are both single layer/multilayer; 8.7/6.3% are single layer/multilayer in MODIS but multilayer/single layer in C-C
- For single-layer cases, ~70% of MODIS low-level clouds are classified as Sc in C-C regardless of optical thickness

Correspondence to:
T. Wang,
Tao.Wang@jpl.nasa.gov

Citation:
Wang, T., E. J. Fetzer, S. Wong, B. H. Kahn, and Q. Yue (2016), Validation of MODIS cloud mask and multilayer flag using CloudSat-CALIPSO cloud profiles and a cross-reference of their cloud classifications, *J. Geophys. Res. Atmos.*, *121*, 11,620–11,635, doi:10.1002/2016JD025239.

Received 15 APR 2016
Accepted 2 SEP 2016
Accepted article online 8 SEP 2016
Published online 1 OCT 2016

Validation of MODIS cloud mask and multilayer flag using CloudSat-CALIPSO cloud profiles and a cross-reference of their cloud classifications

Tao Wang[1], Eric J. Fetzer[1], Sun Wong[1], Brian H. Kahn[1], and Qing Yue[1]

[1]Jet Propulsion Laboratory, California Institute of Technology, Pasadena, California, USA

Abstract Aqua Moderate Resolution Imaging Spectroradiometer (MODIS) Collection 6 cloud observations (MYD06) at 1 km are collocated with daytime CloudSat-Cloud-Aerosol Lidar and Infrared Pathfinder Satellite Observations (CALIPSO) (C-C) cloud vertical structures (2B-CLDCLASS-LIDAR). For 2007–2010, over 267 million C-C cloud profiles are used to (1) validate MODIS cloud mask and cloud multilayer flag and (2) cross-reference between C-C cloud types and MODIS cloud regimes defined by joint histograms of cloud top pressure (CTP) and cloud optical depth (τ). Globally, of total observations, C-C reports 27.1% clear and 72.9% cloudy, whereas MODIS reports 30.0% confidently clear and 58.7% confidently cloudy, with the rest 7.1% as probably clear and 4.2% as probably cloudy. Agreement between MODIS and C-C is 77.8%, with 20.9% showing both clear and 56.9% showing both cloudy. The 9.1% of observations are clear in MODIS but cloudy in C-C, indicating clouds missed by MODIS; 1.8% of observations are cloudy in MODIS but clear in C-C, likely due to aerosol/dust or surface snow layers misidentified by MODIS. C-C reports 47.4/25.5% single-layer/multilayer clouds, while MODIS reports 26.7/14.0%. For C-C single-layer clouds, ~90% of tropical MODIS high (CTP $<$ 440 hPa) and optically thin ($\tau < 3.6$) clouds are identified as cirrus and ~60% of high and optically thick ($\tau > 23$) clouds are recognized as deep convective in C-C. Approximately 70% of MODIS low-level (CTP $>$ 680 hPa) clouds are classified as stratocumulus in C-C regardless of region and optical thickness. No systematic relationship exists between MODIS middle-level (680 $<$ CTP $<$ 440 hPa) clouds and C-C cloud types, largely due to different definitions adopted.

1. Introduction

The global distributions of clouds and their physical and optical properties have been observed by the passive Moderate Resolution Imaging Spectroradiometer (MODIS) on board the Aqua satellite for over 15 years [*King et al*., 1992, 2003, 2013]. Among the large variety of reported cloud properties, the MODIS-derived cloud mask and cloud fractions are widely used in many climate studies [e.g., *Dessler and Yang*, 2003; *Holz et al*., 2008; *Marchand et al*., 2010; *Suzuki et al*., 2010]. In cloudy conditions, cloud top pressure (CTP) and cloud optical thickness (τ) are often used to describe statistical characteristics of different cloud regimes classified in the CTP-τ joint histogram following the conventions of *Rossow and Schiffer* [1999] [e.g., *Marchand et al*., 2010; *Pincus et al*., 2012; *Wong et al*., 2015].

However, MODIS passive imagery of clear and cloudy sky relies largely on the contrast between reflectance from surface and the cloud/aerosols, which results in misidentifications in scenes with a weak contrast from thin clouds or aerosol layers [*King et al*., 2003; *Platnick et al*., 2003]. Moreover, MODIS retrieval of cloud top and τ over integrated paths is based on a single-layer, homogeneous cloud assumption [*Menzel et al*., 2008]. Consequently, applying conventional cloud type definitions from CTP versus τ inevitably leads to ambiguities when multilayer clouds exist [e.g., *Baum and Wielicki*, 1994; *Rossow and Schiffer*, 1999; *Chang and Li*, 2005a, 2005b; *Davis et al*., 2009; *Joiner et al*., 2010; *Mace et al*., 2011]. This has long been an issue before the recent spaceborne active remote sensing by the CloudSat cloud profiling radar [*Stephens et al*., 2002] and the Cloud-Aerosol Lidar and Infrared Pathfinder Satellite Observations (CALIPSO) lidar [*Winker et al*., 2007]. This combined radar-lidar (CloudSat-CALIPSO, hereafter as C-C) data set has provided new opportunities to quantitatively estimate overlapping cloud structures in a wide variety of cloud types, ranging from vertically low to high levels and from optically thin to thick layers [*Mace et al*., 2009]. As C-C and MODIS are in the same A-Train orbit, this enables simultaneous observations of clouds from the perspective of active and passive remote sensing.

Many studies have provided estimates of cloud coverage and cloud overlap based on MODIS and C-C. For example, *Mace et al*. [2009] report global hydrometeor coverage of ~76% from C-C data during July 2006

and June 2007, whereas *King et al*. [2013] reveal the number to be 67% from MODIS. When comparing MODIS and CALIPSO, *Holz et al*. [2008] find the global agreement of >80% for clear and cloudy conditions, although their statistics were based on only 2 months (August 2006 and February 2007). In terms of cloud overlap, *Chang and Li* [2005b] report global rates of cirrus (CTP < 500 hPa, and emissivity < 0.85) overlapping lower level water clouds to be 12.3/12.1% over land/ocean based on 4 months (January, April, July, and October) of daytime Terra/MODIS observations in 2001. By using MODIS multilayer flag [*Wind et al*., 2010], *Joiner et al*. [2010] find that ~10% of cloudy pixels in July 2007 are multilayer—although MODIS multilayer retrieval cannot reveal exactly how many layers of cloud exist. A study based on C-C observations in January, April, July, and October of 2009 indicate the cloud overlap rate in the tropics and midlatitudes to be 12% [*Yuan and Oreopoulos*, 2013], although their results are only limited to two-layer cases.

Besides cloud fraction and overlap, different types of clouds classified by MODIS and C-C are frequently used in climate studies. For example, using cloud types classified by CloudSat, *Jiang et al*. [2011] found that the phase shift (relative to the center of convection) of altostratus (*As*) and altocumulus (*Ac*) during Indian monsoon transitions are primary responsible for the vertical tilting of anomalous cloud fractions. Using MODIS observation of clouds, however, *Wang et al*. [2015] showed that variations of As and Ac during the monsoon transitions are much less than other cloud types. The discrepancies in results are probably due to different definitions of cloud types adopted by C-C and MODIS. Therefore, a cross-reference of the two sets of classification between C-C and MODIS is necessary for our understanding of results using either one of the definitions [e.g., *Li et al*., 2015] and to resolve differences between cloud classification methods in the published literature. This reference provides a "statistical bridge" between C-C cloud types and MODIS cloud regimes.

In this study, we attempt to provide a comprehensive understanding of MODIS observations based on coincident C-C cloud vertical structure from 4 years (2007–2010) of observations. We have three primary goals: (1) MODIS cloud mask at 1 km pixel scale are validated by the C-C observation of clear and cloudy conditions; (2) MODIS multilayer cloud flag (MLF) is validated by the C-C clouds up to five layers; and (3) MODIS *cloud regimes* defined by the CTP-τ joint histogram, as well as cloudy cases that are not associated with τ retrievals, are stratified against C-C *cloud types*. We present statistics of the cloud properties and cloud classification obtained from MODIS as functions of the number of cloud layers and of cloud classification from C-C. We expect these results will be a useful reference for interpreting process studies that use cloud coverage, cloud overlap, and cloud classification from passive MODIS and active C-C.

2. Data Sets and Methodology

The latest version (R04) of the C-C cloud classification product 2B-CLDCLASS-LIDAR [*Wang et al*., 2013] with footprint of approximately 1.7 km along track by 1.4 km across track is currently available for the period of 2007–2010. This product provides vertical profiles of cloud hydrometeors from the synergistic combination of radar (CloudSat) and lidar (CALIPSO). Distinct cloud layers are defined with hydrometeor-free separation of ~480 m [*Marchand et al*., 2008]. At most, 10 layers of clouds are identified, with layer = 0 indicating clear (*Clr*) and with single-layer (*1Lay*, layer = 1) and multilayer (*mLay*, layer > 1) clouds considered cloudy (*Cldy*) *condition*. In this study we only show C-C clouds up to five layers, because the cases of more than five layers of clouds are less than 0.06% of total observations. For each cloud layer, the algorithm provides cloud base/top heights and a unique *cloud type* from rule-based and fuzzy-logic-based classifications by using many cloud properties such as height, temperature, thermodynamic phase, thickness, cloud cover, cloud homogeneity, cloud horizontal extent, and the presence or absence of precipitation (refer to *Wang et al*. [2013] for details). There are eight basic cloud types defined: cirrus (*Ci*), altostratus (*As*), altocumulus (*Ac*), stratus (*St*), stratocumulus (*Sc*), cumulus (*Cu*), nimbostratus (*Ns*), and deep convection (*DC*). Cloud top/base pressures are obtained from the auxiliary European Center for Medium-Range Weather Forecasting (ECMWF) reanalysis product ECMWF-AUX [*Partain*, 2007] that provides atmospheric state variables interpolated from the nearest ECMWF grid point. Figure 1a illustrates a diagram of the C-C data structure used in this investigation.

Aqua MODIS Collection 6 (MYD06) Level 2 (L2) 1 km cloud mask, cloud top pressure (CTP), and cloud optical thickness (τ) [*Baum et al*., 2012; *Platnick et al*., 2013, 2015] during daytime are used for the same C-C period of 2007–2010. By using geolocation fields (MYD03) in 1 km, we collocate each daytime MODIS 1 km scene of CTP and τ to its closest C-C footprint within 1 km at local time. For the entire 2007–2010 record, over 75% of the

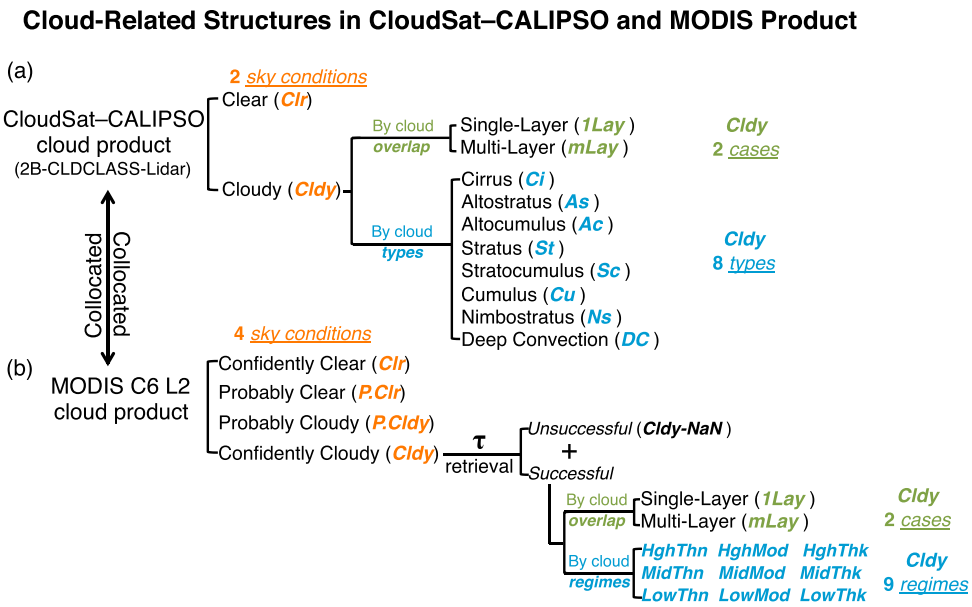

Figure 1. The data structures in terms of clear/cloudy (Clr/Cldy) conditions, single-layer/multilayer (1Lay/mLay) cases, and cloud classifications in (a) CloudSat-CALIPSO (C-C) product (2B-CLDCLASS-LIDAR) and (b) MODIS Collection 6 L2 product. Italic-bold words are the acronyms used in this study. Note that the two products are one-to-one collocated at pixel scale within 1 km (among them, >75% are within 0.5 km distance) so that the four MODIS Clr/Cldy conditions consume all C-C measurements. See context for more details.

collocated pixels/footprints are separated within 0.5 km distance and over 93% are within 0.6 km. This correspondence guarantees the most accurate comparison with the smallest spatial and temporal sampling biases. We examine C-C cloud profiles under MODIS conditions of confidently clear (Clr), probably clear (P.Clr), probably cloudy (P.Cldy), and confidently cloudy (Cldy) based on the MODIS cloud mask cloudiness flags. Therefore, scenes with MODIS Clr but C-C Cldy contain clouds missed by MODIS; whereas scenes showing MODIS Cldy but C-C Clr indicate clouds misidentified by MODIS.

Under Cldy conditions when τ is available, MODIS multilayer flag (MLF) [*Wind et al*., 2010; *Platnick et al*., 2015] retrieved on pixel scale is also used to differentiate single-layer (1Lay, MLF = 1) and multilayer (mLay, MLF $\geq$ 2) *cases*. The MLF has recently being updated by including the *Pavolonis and Heidinger* [2004] algorithm for general purpose cloud overlap detection. The MODIS MLF essentially identifies cases when a thin ice cloud is above a thicker liquid cloud, for which the total integrated water vapor amount above cloud tops computed from the infrared CO_2-slicing method would be inconsistent with the total amount retrieved from using the near-infrared reflectance differences at the 0.86 and 0.94 μm (because water vapor is the main absorber at 0.94 μm). When the inconsistency reaches more than 8% of the total integrated water vapor amount, the MODIS pixel is flagged as *potentially* containing multilayer clouds [*Joiner et al*., 2010]. That said, the MODIS MLF relies largely on the failure of the single-layer, plane-parallel, and homogeneous assumption of the cloud effective radius retrieval, because of the presence of two distinct cloud layers with different thermodynamic phases. As mentioned in *Wind et al*. [2010], MLF is not designed to detect every instance of multilayer clouds. In contrast, C-C can identify all kinds of multilayer cases, even with two thin layers of cirrus on top of each other. We emphasize that the C-C single-layer and multilayer results should be taken as truth when comparing to MODIS MLF.

Under Cldy conditions when τ is available, a total of nine MODIS cloud regimes following the International Satellite Cloud Climatology Project (ISCCP) CTP-τ joint histogram convention [*Rossow and Schiffer*, 1999] will be compared directly with the C-C cloud types. MODIS CTP is obtained from a combined CO_2-slicing method using 13.3–14.2 μm infrared band for middle- to high-level clouds and the infrared window approach at 11 μm for low-level clouds [*Menzel et al*., 2015]. The MODIS CTP tends to be the pressure of the top-layer cloud visible to integrated optical depths greater than unity [*Menzel et al*., 2008]. MODIS cloud optical properties are retrieved from MODIS multispectral reflectance [*Platnick et al*., 2015], and they tend to be the thickness of the

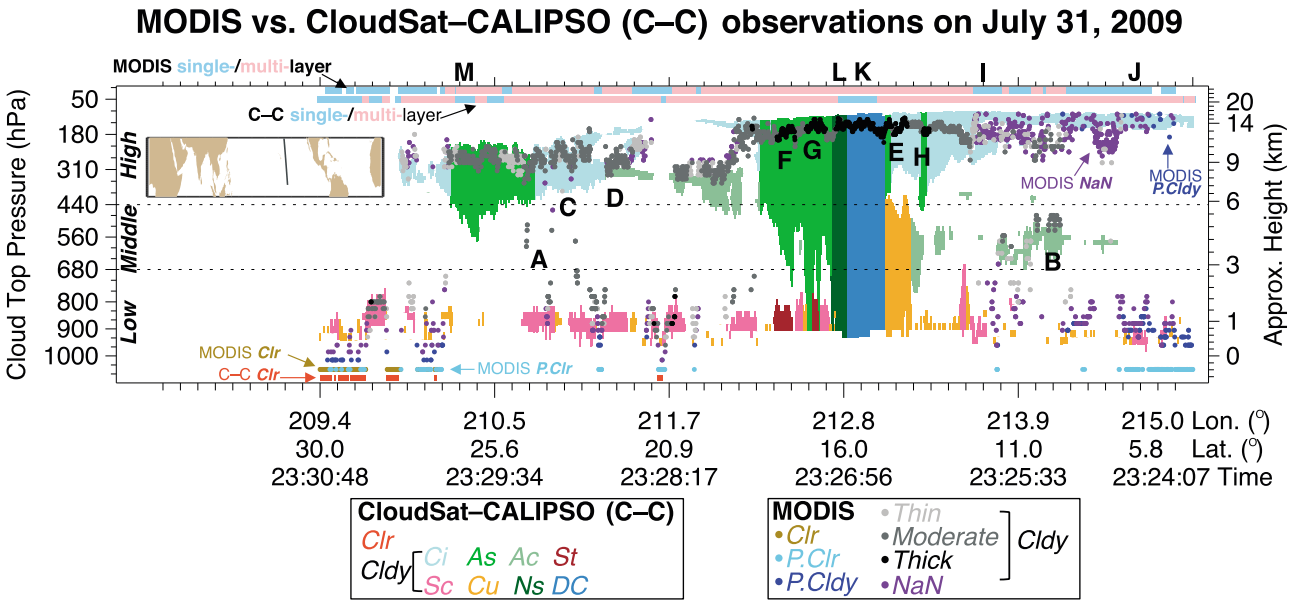

Figure 2. Curtain plot of different cloud types classified by CloudSat-CALIPSO (C-C, shaded color), compared to MODIS cloud top (dots). Following the ISCCP convention of using 680 hPa and 440 hPa (dotted grey lines) to separate low-, middle-, and high-level clouds, nine basic MODIS cloud regimes can be determined with MODIS cloud optical depths (τ) from thin (light grey) to thick (black). Colored dots denote MODIS clear (Clr, dark yellow), probably clear (P.Clr, cyan), probably cloudy (P.Cldy, blue), and cloudy without τ retrievals (NaN, purple). The horizontal bars at the top indicate single-layer/multilayer (light blue/pink) flags from MODIS (first bar) and from C-C (second bar), respectively.

whole column. Ranging vertically over low ($1000 \leq CTP < 680$ hPa, "Low"), middle ($680 \leq CTP < 440$ hPa, "Mid"), and high ($440 \leq CTP < 50$ hPa, "Hgh"), and optically over thin ($0 < CTP < 3.6$, "Thn"), moderate ($3.6 \leq CTP < 23$, "Mod"), and thick ($23 \leq CTP < 200$, "Thk"), the MODIS nine cloud regimes are referred as *LowThn*, *LowMod*, *LowThk*, *MidThn*, *MidMod*, *MidThk*, *HghThn*, *HghMod*, and *HghThk*, respectively. Note that the MODIS definitions of cloud regimes are from the radiative point of view, whereas the C-C cloud types are from the morphological point of view. Therefore, we provide a direct cross-reference of the two but with no suggestion of which classification is superior to another.

Moreover, there exist cases of MODIS Cldy but with no τ retrievals denoted as Cldy-NaN, representing the low-quality cloud property retrievals [*Marchand et al.* [2010]]. Those might be caused by surface glint, heavy dust or smoke contamination, cloud edges, or partly cloudy pixels [*Platnick et al.*, 2015]. The detailed structure of the MODIS data set is depicted in Figure 1b.

Vertical cloud structures in C-C are then stratified against each MODIS observational condition, case, and cloud regime. In this paper, C-C cloud structures are considered as a reference for "truth" in validating MODIS clear/cloud conditions and cloud overlap. No analogous "truth" references for cloud types exist, however, because they are inherently more ambiguous and are defined differently among observing techniques. Regardless, we attempt to determine the relative rate of equivalence between the two data sets to bridge our understanding of results using the two sets of classifications [e.g., *Jiang et al.*, 2011; *Wang et al.*, 2015]. The focus is restricted to daytime observations only when MODIS cloud optical properties are available. Approximately 200,000 coincident MODIS pixels and C-C footprints are examined globally each day, for a total of over 267 million pixels in the 4 years 2007–2010 (excluding a few missing time segments), ensuring robust global statistics.

3. Results

3.1. An Example of Cloud Observations by the Two Sensors

Figure 2 is a curtain plot along a path over the Eastern Pacific Ocean (see inset map) on 31 July 2009, demonstrating how differently the MODIS and C-C observe clouds. C-C cloud types are shaded in different colors, together with MODIS cloud top marked from light grey to black dots representing optically thin to thick

clouds. MODIS Clr/P.Clr (dark yellow/cyan dots) and C-C Clr (orange shading) are vertically stacked below the surface for easy visualization. MODIS P.Cldy (blue dots) and Cldy-NaN (purple dots) represent part of the uncertainties in retrieving cloudy pixels.

The morphology of MODIS clouds generally agrees with the C-C observations. Particularly, most of the MODIS cloud tops are consistent with C-C but at slightly lower altitudes. This is because MODIS detects cloud tops at integrated optical depths greater than unity [*Menzel et al.*, 2008]; hence, the radiative cloud top in MODIS is always lower than the physical cloud top detected by C-C [*Mace et al.*, 2011]. Moreover, MODIS infrared radiances occasionally provide cloud top in-between cloud layers when the upper level clouds are relatively thin and semitransparent to MODIS (A in Figure 2); when the upper level clouds are thin enough to be transparent to MODIS, the retrieved cloud tops fall closer to the tops of lower level clouds (B in Figure 2).

The existence of overlapping clouds brings challenges in retrievals of not only cloud top but also cloud thickness; therefore the MODIS cloud regimes based on CTP-τ classification using radiative cloud tops will yield some uncertainties. For example, when high and thin clouds are above low-level thin clouds (C and D in Figure 2), MODIS suggests the whole column as high- and moderately thick clouds (HghMod). In cases of high and thin clouds above middle-level clouds (E in Figure 2), or high and thick clouds above low-level clouds (F and G in Figure 2), MODIS suggests the whole column as high-thick clouds (HghThk). Similar cases can also be found for three layer clouds (H in Figure 2). A primary objective of this investigation is to determine how frequently the MODIS cloud classification misidentifies the scene.

Collocation between MODIS and C-C allows us to validate the MODIS MLF [*Wind et al.*, 2010; *Platnick et al.*, 2015] by comparing it to the single-layer (light blue) and multilayer (pink) detections in C-C as shown at the top of Figure 2. Since the MODIS MLF algorithm is only triggered when clouds with $\tau > 4$ are detected [*Wind et al.*, 2010; *Joiner et al.*, 2010], all MODIS clouds with $\tau \leq 4$ are considered single layer. This leads to misclassification of multilayer thin clouds as single layer (I and J in Figure 2) and single-layer thick clouds as multilayer (K, L, and M in Figure 2) in MODIS.

In Figure 2 we also see that the C-C classified Ac and As can extend much higher in altitude, because the C-C classification of clouds, especially the middle-level ones, has a different physical basis from the radiative definitions of cloud regimes in MODIS. For example, the Ac in C-C refers to clouds of middle base, or clouds of low base and middle top; while the As refers to clouds of middle base, or clouds of low base and middle to high top [*Wang and Sassen*, 2001; *Wang et al.*, 2013]. Therefore, caution should be taken when cross-referencing results of cloud type classifications in studies using passive imagers (e.g., ISCCP or MODIS) and active sensors (e.g., C-C).

The 4 year global statistics comparing MODIS and C-C cloud conditions and MLF, as well as statistical relationships of cloud classifications, will be further discussed in sections 3.2 and 3.3, respectively.

3.2. Validation of MODIS Cloud Mask and Multilayer Flag (MLF)

Figure 3a summarizes the occurrence frequencies of different clear/cloudy conditions and single-layer/multilayer ratios in MODIS (open circle) and in C-C (open diamond) separated by different latitudinal bands (30°N–S for tropics, 30–60°N–S for midlatitudes, and 60–90°N–S for high latitudes). Here cloudy conditions are with respect to total observations, so for MODIS (Clr + P.Clr + P.Cldy + Cldy) = 100% and for C-C (Clr + Cldy) = 100%. On the right side of the vertical dashed line are the ratios of single-layer (1Lay) and multilayer (mLay) cases with respect to total Cldy conditions, so that for MODIS (1Lay + mLay + NaN) = Cldy and for C-C (1Lay + mLay) = Cldy.

Overall, 30.0% and 58.7% of MODIS observations are reported confidently Clr and Cldy, respectively [cf. *King et al.*, 2013]; whereas in C-C the numbers are 27.1% and 72.9% [cf. *Mace et al.*, 2009, respectively, with slightly higher cloud fractions due to its higher sensitivity. Differences between the two can be partially attributed to the 4.2% of P.Cldy condition in MODIS. The rest of the difference (7.1% of P.Clr in MODIS) can be partially attributed to the fact that the MODIS cloud retrieval algorithm attempts to eliminate pixels around cloud edges and pixels containing both clouds and aerosols [e.g., *Joiner et al.*, 2010; *King et al.*, 2013]. On average, the tropics have at least 10% more Clr than the midlatitudes, mostly due to the subsiding branch of the Hadley circulation over the mostly clear subtropics. Cldy over the midlatitudes is 10% more than over the tropics in C-C (20% more in MODIS)—mainly due to ubiquitous clouds in the storm tracks.

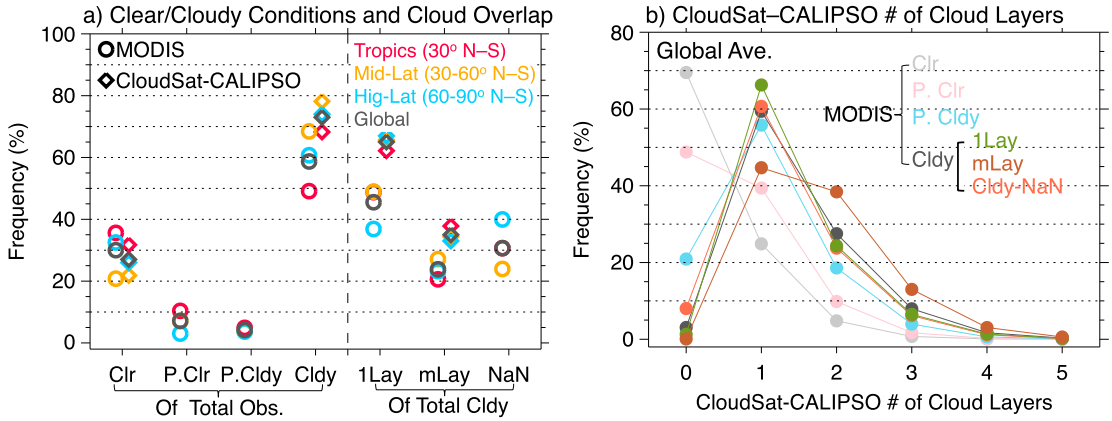

Figure 3. (a) Occurrence frequencies of clear/cloudy (Clr/Cldy) conditions with respect to total observations (>267 million in 2007–2010) for MODIS (open circle) and CloudSat-CALIPSO (C-C, open diamond) over different latitudinal regions. Here all Clr/Cldy conditions sum to the total number of observations, so MODIS (Clr + P.Clr + P.Cldy + Cldy) = 100%, and C-C (Clr + Cldy) = 100%. On the right side of the vertical dash line are the fractions of single-layer (1Lay) and multilayer (mLay) cases with respect to total cloudy conditions, so that MODIS (1Lay + mLay + NaN) = Cldy and C-C (1Lay + mLay) = Cldy. (b) Histograms of number of cloud layers detected by C-C under different MODIS Clr/Cldy conditions and MODIS Cldy multilayer flag.

Occurrences of single-layer and multilayer clouds are compared on the right side of Figure 3a. Of the total Cldy in C-C (72.9% of total global observations), 65.0% are determined as single-layer and 35.0% as multilayer due to its better sensitivity of cloud vertical structures [e.g., *Winker et al*., 2007; *Li et al*., 2015]. Of the total Cldy in MODIS (58.7% of total global observations), 45.5% are flagged as single-layer and only 23.9% are flagged as multilayer; the rest 30.6% are Cldy-NaN. With respect to total observations, C-C single-layer and multilayer rates are therefore 47.4% (65.0% × 72.9%) and 25.5% (35.0% × 72.9%), respectively; whereas MODIS rates are 26.7% (45.5% × 58.7%) and 14.0% (23.9% × 58.7%), respectively.

Those results are roughly referenced to other studies listed in Table 1. We see that C-C global cloud-overlap rate of 25.5% is in stark contrast to the 12% in *Yuan and Oreopoulos* [2013], likely because our calculation of cloud-overlap includes two or more cloud layers globally for 2007–2010, whereas the *Yuan and Oreopoulos* [2013] only considered two-layer cases constrained within 60°N–S for January, April, July, and October of 2009. Separating C-C global overlap rates into cases of two, three, four, and five layers, the occurrence frequencies are 19.1%, 5.2%, 1.0%, and 0.2%, respectively. Meanwhile, our cloud overlap rates obtained from MODIS (14.0%) is close to the 12.2% reported in *Chang and Li* [2005b], although the two studies investigated overlapping clouds by applying different algorithms in different periods of time. Moreover, two studies used different data sets that capture different low cloud amounts due to its strong diurnal variation— for Aqua/MODIS crossing time of 1:30 pm, there could be on the order of ~10% less low clouds than on the Terra/MODIS crossing time of 10:30 am [e.g., *Klein et al*., 1995].

Since the MODIS multilayer algorithm categorizes all clouds of $\tau \leq 4$ as single layer, MODIS reports more single-layer cases in the tropics where thin multilayer clouds (such as I and J in Figure 2) are commonly present [e.g., *Yuan and Oreopoulos* 2013; *Li et al*., 2015]. This is the primary cause of the discrepancy with C-C observations that have the most frequent multilayer clouds in the tropics. Over higher latitudes, MODIS reports less frequent single-layer cases, probably because of frequent single-layer thicker clouds that are miscategorized as multilayer. C-C shows smaller regional variations (less than 1–5%) in cloud overlap.

Each MODIS observational condition is stratified against the C-C number of cloud layers that adds up to 100% in Figure 3b. Here layer = 0 represents clear sky; and layer = 1 and layer > 1 are single-layer and multilayer clouds, respectively. When MODIS observes Clr (grey), ~70% of them are also flagged as clear in C-C (layer = 0). The remainders are single-level (~25%) cirrus or low-level broken clouds as seen in *Pincus et al*. [2012], suggesting limitations of MODIS in detecting thin and low clouds. Occasionally, these could also be multilayer thin clouds (<5%). There is also the possibility that the discrepancies arise from the collocation in which the MODIS fields of view are partially filled by the C-C pixels. Under the MODIS Cldy condition (charcoal), 4%, 60%, 28%, and 8% of the occurrences are clear, single-, two-, and three-layer clouds, respectively in C-C. About 67% of MODIS single-layer (green) cloudy detections agree with their counterparts in C-C; whereas the rest are identified as two- (25%) and three-layer (8%) clouds by C-C. Among the MODIS multilayer clouds

Table 1. Comparing the Absolute (With Respect to Total Observations) and Relative (With Respect to Cloudy Scenes) Fractions of Multilayer Clouds in Different Studies[a]

			This study	
Study	*Chang and Li* [2005b]	*Yuan and Oreopoulos* [2013]	CloudSat-CALIPSO (C-C)	MODIS
Absolute fraction	12.2%	12.0%	25.5%	14.0%
Relative fraction[a]	27.3% (relative to 44.8% overcast scenes)	29.7% (relative to 40.4% low cloud fraction in Jan 2009)	35.0% (relative to 72.9% cloudy footprints)	23.9% (relative to 58.7% confidently cloudy pixels)
Time and domain	Jan, Apr, Jul, and Oct 2001; global	Jan, Apr, Jul, and Oct 2009, 60°N–S	2007–2010; global	2007–2010; global
Input data	Terra/MODIS Collection 4 MOD02, MOD35, and MOD06; daytime only	R04 2B-GEOPROF-Lidar, 1.7 km × 1.4 km, CALIOP CLay, 1 km *Mace et al.* [2009]	R04 2B-CLDCLASS-Lidar, 1.7 km × 1.4 km; daytime only	Aqua/MODIS Collection 6 MYD06, 1 km, daytime only (matched to C-C) *Wind et al.* [2010] and *Platnick et al.* [2015]
Algorithm	*Chang and Li* [2005a]	and *Vaughan et al.* [2004]	*Wang et al.* [2013]	
Note	Examine cases of semitransparent high cirrus (CTP < 500 hPa, emissivity < 0.85) on top of lower level water clouds	Examine cases of high cloud (base > 5 km local topography or > 7 km sea level) above low cloud (top ≤ 3.5 km)	Examine footprints of layer numbers (≥2); different layers are separated ~480 m.	Examine multilayer flag (MLF) in each pixel

[a]Note that the relative fractions are with respect to cloudy population defined differently.

(brown), 55% of them are also recognized as multilayer, but the most (45%) are considered single layer in C-C. MODIS histograms of P.Clr and P.Cldy basically mirror that of Clr and Cldy, respectively, indicating that these two categories are skillful.

The relationships between MODIS and C-C observations are best summarized using a confusion matrix listed in Table 2. Here C-C observations are stratified against each of the MODIS Clr, P.Clr, P.Cldy, and Cldy conditions and Cldy single-layer and multilayer cases. Different from previous statistics, here all reported fractions are relative to the total >267 million observations in 2007–2010. Numbers within C-C Cldy1Lay, CldymLay and MODIS Cldy1Lay, CldymLay, Cldy-NaN are the general Clr/Cldy statistics that add up to 100% of total measurements; the sum of each column and each row is the total fraction of each scenario for MODIS and C-C, respectively. For example, C-C Clr = (20.9 + 3.5 + 0.9 + 1.8)% = 27.1%, and MODIS Clr = (20.9 + 9.1)% = 30%. Similarly, C-C Cldy = (9.1 + 3.6 + 3.3 + 56.9)% = 72.9%, and MODIS Cldy = (1.8 + 56.9)% = 58.7%. Among them, numbers in bold are scenarios when both sensors observe Clr (20.9%) and Cldy (56.9%), which sum to the 77.8% rate of total agreement (close to the results by *Holz et al.* [2008] that compared MODIS with CALIPSO for August 2006 and February 2007). Similarly, diagonal elements within C-C Cldy1Lay, CldymLay and MODIS Cldy1Lay, CldymLay, Cldy-NaN are scenarios when both sensors detect 1Lay (17.7%) and mLay (7.7%) clouds, constituting an overall agreement of 25.4% for cloud overlap. All other off-diagonal elements are disagreements, with major ones (Clr versus Cldy and 1Lay versus mLay) *underlined*. Note that Cldy(1Lay + mLay) = total Cldy for C-C, and Cldy(1Lay + mLay + NaN) = total Cldy for MODIS.

Previous works have reported the level of agreement with respect to spatial distributions of clouds observed simultaneously by MODIS and Cloud-Aerosol Lidar with Orthogonal Polarization (CALIOP) on board of CALIPSO [e.g., *Holz et al.*, 2008]. Thus, we now focus on the level of disagreement between the two sets of observations. Figure 4 shows Clr/Cldy conditions when MODIS disagrees with C-C. We see that the scenario of C-C Clr and MODIS Cldy (Figure 4a) is seasonally dependent. During boreal winter (December–February, DJF), aerosols due to coal burning in northeast China and extremely cold surface air over northern Canada, the Arctic Ocean, and Greenland are occasionally considered cloudy by MODIS [e.g., *Frey et al.*, 2008]. During boreal spring (March–May, MAM) and summer (June–August, JJA) in regions where dust outflow is strong (e.g., tropical Eastern Atlantic), there is a tendency for MODIS to

Table 2. Global Occurrence Frequencies of MODIS and CloudSat-CALIPSO Cloud Scenarios and Multilayer Flag Cases With Respect to Total 267,402,526 Observations[a]

	MODIS						
C-C	Clr	P.Clr	P.Cldy	Cldy	Cldy1Lay	CldymLay	Cldy-NaN
Clr	**20.9%**	3.5%	0.9%	*1.8%*	0.3%	0.0%	1.5%
Cldy	*9.1%*	3.6%	3.3%	**56.9%**	26.4%	14.0%	16.5%
Cldy1Lay	7.4%	2.8%	2.3%	34.9%	**17.7%**	*6.3%*	10.9%
CldymLay	1.7%	0.8%	1.0%	22.0%	*8.7%*	**7.7%**	5.6%

[a]All percentages are with respect to total observations. Percentages within C-C Clr and Cldy and MODIS Clr, P.Clr, P. Cldy, and Cldy add up to be 100%. Add up of each column and each row is the total fractions of each scenario for MODIS and C-C, respectively. For example, C-C total clear (Clr) = (20.9 + 3.5 + 0.9 + 1.8)% = 27.1%; MODIS total Clr = (20.9 + 9.1)% = 30%. Similarly, C-C total cloudy (Cldy) = 72.9% and MODIS Cldy = 58.7%. Bold numbers are the major agreements between MODIS and CloudSat-CALIPSO (C-C). In terms of cloud mask, the total agreement is 77.8%, with 20.9% showing both clear (Clr) and 56.9% showing both cloudy (Cldy); in terms of single/multilayer clouds the agreement is 25.4%, with 17.7% showing both single-layer (Cldy1Lay) and 7.7% showing both multilayer (CldymLay). *Italic numbers* are the *major* disagreements between MODIS and C-C. Under each row of C-C scene, MODIS (Cldy1Lay + CldymLay + Cldy-NaN) = MODIS Cldy; under each column of MODIS scene, C-C (Cldy1Lay + CldymLay) = C-C Cldy.

identify pixels as cloudy. There is also a large area over the Eastern Antarctic where MODIS tends to assume that cloudy but C-C flags clear during boreal spring and fall (September–November, SON) [e.g., *Bromwich et al.*, 2012]. Note that for most of those misidentified clouds by MODIS, no valid τ were retrieved.

A total of 9.1% observations are Cldy in C-C but Clr in MODIS. C-C reveals that >80% of those scenes are single-layer Ci (29%), Cu (24%), Sc (22%), or Ns (5%). Those are less seasonally dependent (Figure 4b), and they imply limitations of MODIS to observe either thin Ci ($\tau < 0.3$, somehow transparent to MODIS) or low-level broken clouds such as Cu [e.g., *Pincus et al.*, 2012]. Disagreement arises in the Polar Regions where surface snow coverage or sea ice reduces the contrast between targets (clouds) and the background (surface), resulting in more Clr pixels in MODIS [*Holz et al.*, 2008].

Figure 5 shows the single-layer/multilayer clouds when MODIS disagrees with C-C. The scenario of C-C single-layer and MODIS multilayer (Figure 5a) frequently occurs over the deep tropics (e.g., single-layer, thick column of deep convective (DC) clouds labeled as K in Figure 2), the Tibetan Plateau, and the poleward side of the southern ocean storm track, where clouds are frequently thick and vertically extended such that the MODIS MLF algorithm tends to flag them as multilayer. It is found that a large portion of those cases are when C-C observes single-layer Ns (such as L in Figure 2), As (M in Figure 2), or Ac. In the scenario of C-C multilayer and MODIS single layer (Figure 5b), these are prevalent thin Ci overlaying deep convective clouds in Intertropical Convergence Zone (such as I and J in Figure 2).

3.3. MODIS Cloud Regimes and CloudSat-CALIPSO Cloud Types

Many studies evaluate the differences of cloud heights by active and passive sensors [e.g., *Holz et al.*, 2008; *Kahn et al.*, 2008; *Joiner et al.*, 2010]. Here in Figure 6 we show the joint histograms of MODIS CTP and C-C top-layer CTP for each MODIS cloud regime over the tropics. When MODIS detects high-level clouds (Figures 6a–6c), they are almost always high clouds in C-C. When MODIS detects low-level clouds (Figures 6g–6i), they are mostly low-level or high-level clouds (transparent to MODIS) in C-C, with a smaller contribution from middle-level clouds. The most ambiguous situation is when MODIS observes middle-level clouds (Figures 6d–6f), where C-C assigns the clouds at any altitude with almost uniform probability. Recall that some MODIS Cldy pixels have no accompanying optical depth retrievals; thus, we include the Cldy-NaN in Figure 6j to show the remaining population, demonstrating ubiquitous features over the tropics rather than caused by particular cloud types. Similar results can be found in midlatitudes and high latitudes, with slightly lower cloud tops for middle- and high-level clouds in general.

The occurrence frequencies of each MODIS cloud regime with respect to total Cldy scenario (open circles on the left of vertical dashed lines) are shown in Figure 7. The Cldy-NaN (purple, 25–40% of MODIS total Cldy) is included so that with the nine cloud regimes add up to 100% of total Cldy. Then for each MODIS regime, normalized histograms of the number of cloud layers determined from C-C are shown for the tropics (Figure 7a), midlatitudes (Figure 7b), and high latitudes (Figure 7c). MODIS always observes slightly more frequent LowMod (pink) and HghMod (blue) clouds than the other cloud regimes. In the tropics, the

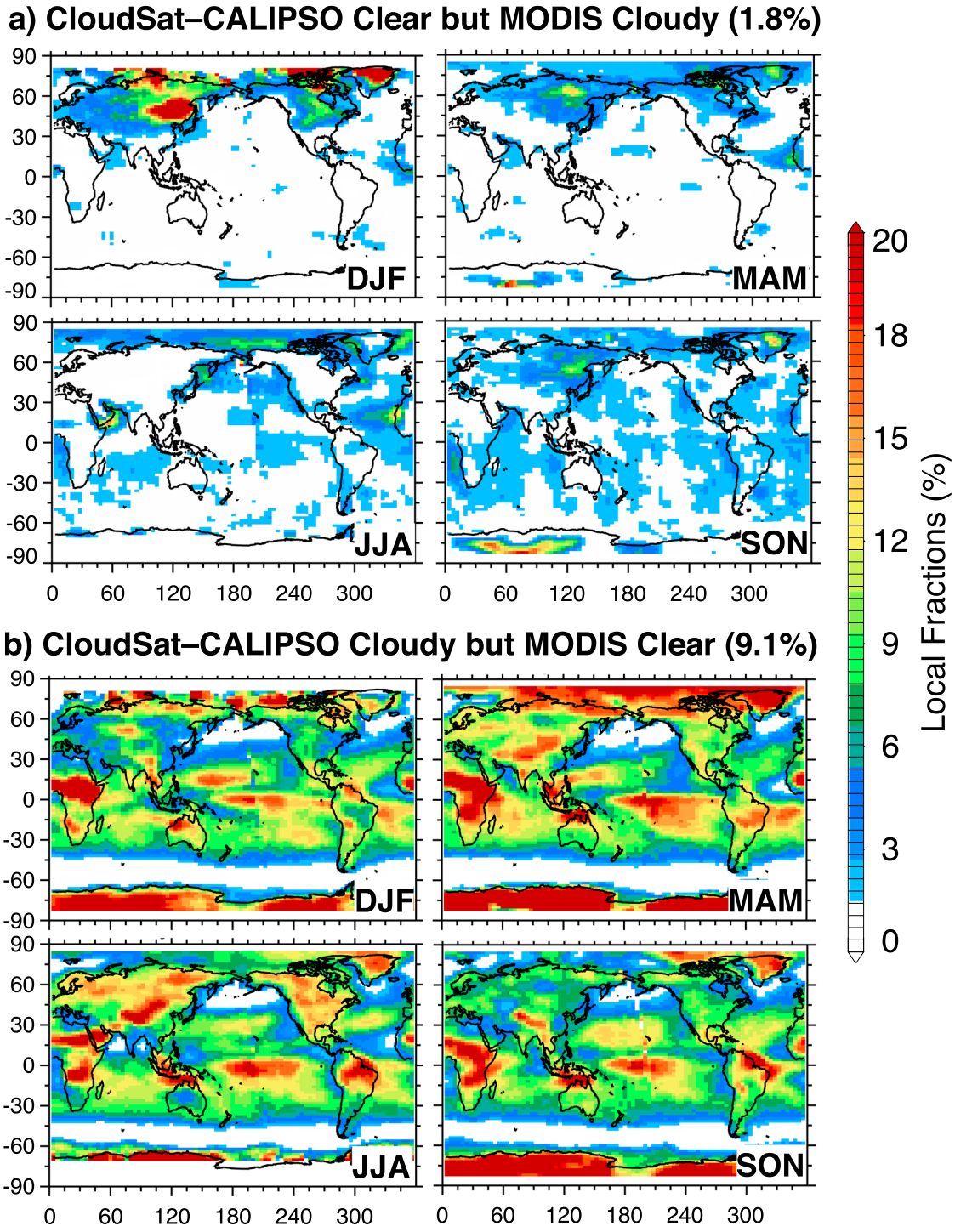

Figure 4. Seasonal distributions of clear/cloudy conditions when MODIS disagrees with CloudSat-CALIPSO (C-C) for 2007–2010. (a) C-C clear but MODIS cloudy and (b) C-C cloudy but MODIS clear. The local fractions are relative to total observations within each 4° × 2° longitude by latitude box. The global and annual averages are shown in the panel titles.

HghThn clouds (light blue) are at least 18% of total Cldy, while in higher latitudes the percentages decrease dramatically to less than 4%. Clouds are most often found to be single layer, except for the HghMod (blue) regime over the tropics that is single layer or two layer with equal probability. Less than 2% of clouds have more than three layers, so our remaining focus will be on clouds that have up to three layers.

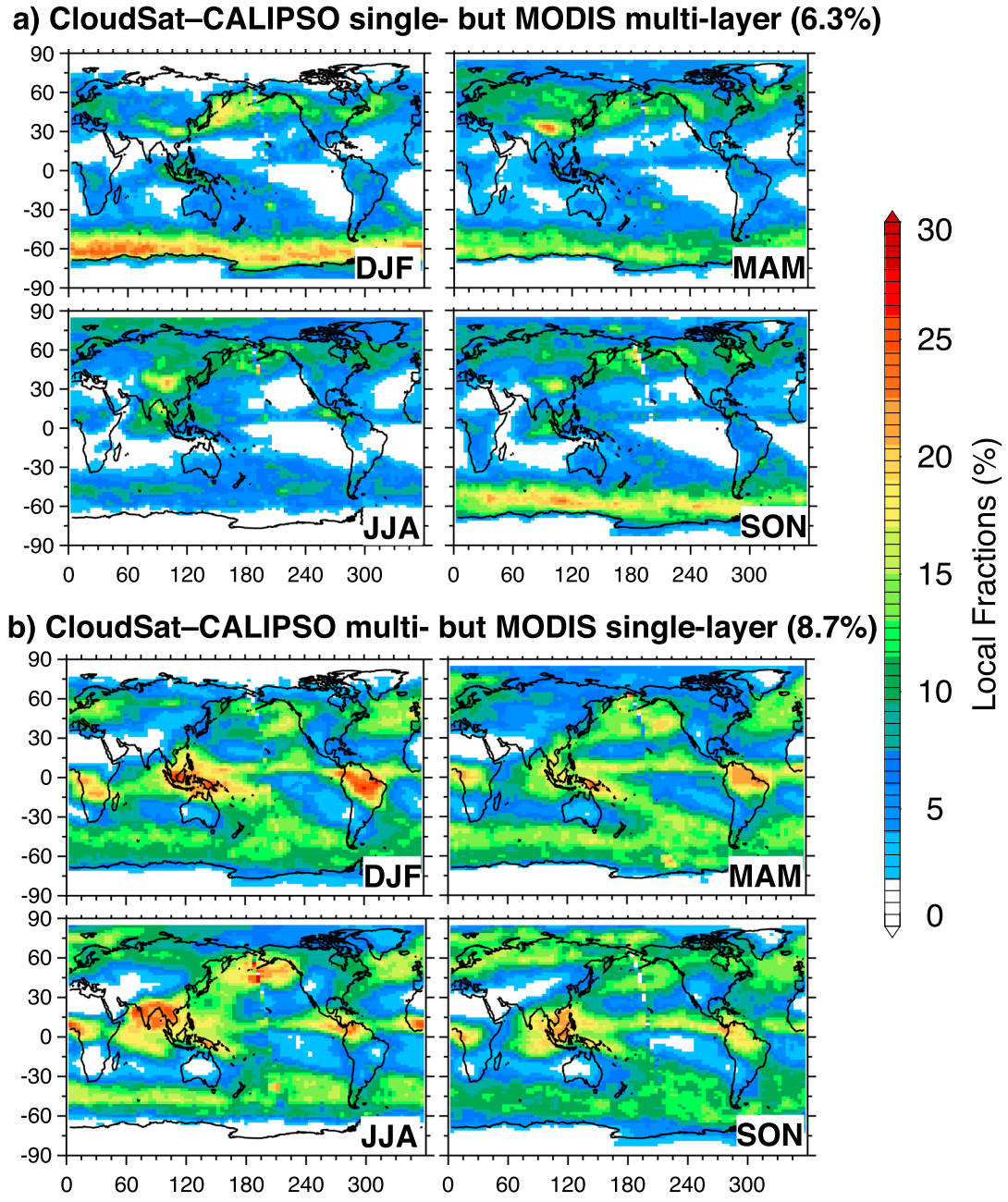

Figure 5. Seasonal distributions of single-layer/multilayer clouds when MODIS disagrees with CloudSat-CALIPSO (C-C) for 2007–2010. (a) C-C single layer but MODIS multilayer and (b) C-C multi but MODIS single layer. The local fractions are relative to total observations within each 4° × 2° longitude by latitude box. The global and annual averages are shown in the panel titles.

Due to the single-layer cloud assumption in MODIS retrievals [*Menzel et al.*, 2008], a fair cross-reference of MODIS cloud regimes to C-C cloud types is for single-layer clouds identified by C-C, as shown in Figure 8. The numbers in Figure 8 are also listed in Table 3 for clear quantification. We can see clearly that more than 70% of MODIS low-level clouds (below 680 hPa level) are consistently classified as Sc in C-C, regardless of their optical thickness. About 90% of MODIS tropical HghThn clouds (light blue) are consistently identified as Ci in C-C. This consistency reduces to 51% in the midlatitudes with most of the remainder (42%) identified as As and a further reduction to 16% in high-latitudes where the remaining 54% are As and 26% are Ns. In the tropics, most MODIS HghMod clouds (blue) are identified as either As (41%) or Ci (30%); whereas in middle- and high-latitude MODIS HghMod clouds are preferentially classified as As (44% and 30%, respectively) or Ns

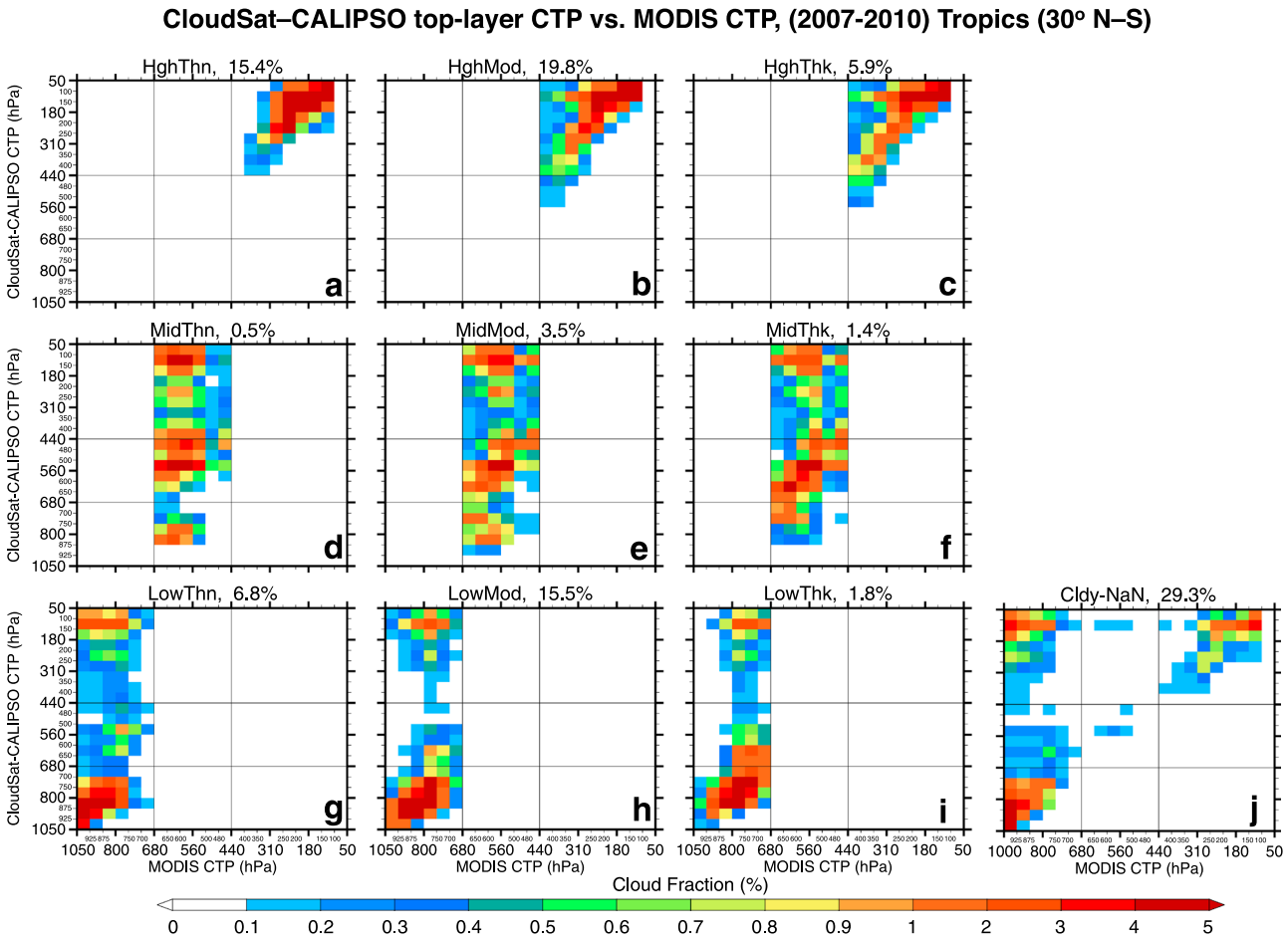

Figure 6. Joint histograms of MODIS cloud top pressure (*x* axis) and CloudSat-CALIPSO (C-C) top-layer cloud top pressure (*y* axis) in different MODIS cloud regimes (including Cldy-NaN) when *both observe clouds* in the tropics (30°N–S). Statistics are for 2007–2010, with each panel normalized so that fractions in all 21 × 21 pressure bins sum to 100%.

(35% and 63%, respectively). Note that in the C-C cloud-type classification, there is no cirrostratus type (equivalent to our HghMod) as with ISCCP classification. About 60% of tropical MODIS HghThk (dark blue) clouds are identified as DC in C-C. In midlatitude and high latitude the numbers drop to only 11% and 2%, respectively, with most of the remainder (>60%) classified as Ns.

While most low- and high-level cloud types are consistently related between MODIS cloud regimes and C-C cloud classifications, the relationships for middle-level clouds are most uncertain. Over the tropics, the majority of MODIS middle-level clouds are recognized as Ac, Sc, or Cu, while over the higher latitudes the middle-level clouds are identified as a variety of cloud types in C-C. This reaffirms a note of caution that the classifications depend on different definitions of middle-level clouds. Different from MODIS middle-level clouds defined by cloud top ($440 < \mathrm{CTP} \leq 680$ hPa), the Ac or As in C-C could be clouds of middle base, clouds of low base and middle top, or clouds of low base and middle/high top [*Wang and Sassen*, 2001; *Wang et al.*, 2013]. Besides physical cloud top/base heights, the C-C cloud classifications are also determined by other cloud properties such as thermodynamic phase, spatial homogeneity, and the presence or absence of precipitation.

Although occurring less frequent than single-layer clouds, multilayer clouds (globally 35% of total cloudy according to C-C, Figure 3a) are critical for our understanding of the radiative impacts of different cloud types [e.g., *Chang and Li*, 2005a; *Li et al.*, 2015]. We then ask the question; "what are the vertical distributions of C-C cloud types in the case of multilayer clouds?" Figures 9a and 9c show the histograms of C-C cloud types when MODIS identifies HghThn clouds while two and three layers of clouds are actually present. The first impression is the ubiquitous Ci [e.g., *Sassen and Mace*, 2002; *Wang and Dessler*, 2012] found at the upper layer.

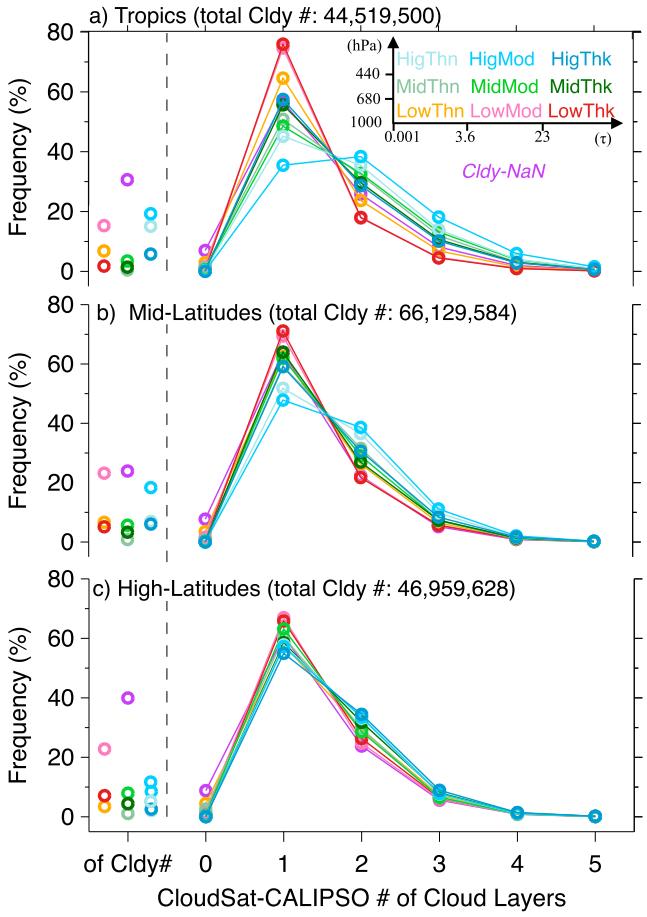

Figure 7. Histograms of CloudSat-CALIPSO (C-C) number of cloud layers for different MODIS cloud regimes in (a) the tropics (30°N–S), (b) the midlatitudes (30–60°N–S), and (c) the high latitudes (60–90°N–S) in 2007–2010. Colored circles on the left of the vertical dashed lines are occurrence frequencies of each regime relative to total cloudy conditions. The histogram for each cloud regime in each region is normalized to 100%.

When MODIS observes tropical (red) HghThn clouds (Figures 9a and 9c), the upper layer clouds are consistently recognized as Ci by C-C; occasionally, the upper layer clouds can also be identified as As in higher latitudes. Below the upper layer, clouds can be recognized as a variety of cloud types by C-C.

The vertical structure is even more complicated when MODIS detects HghThk clouds. For two-layer cases (Figure 9b), ~30% of tropical clouds (red) at low level are classified as DC in C-C; the remainder are Ns, Ac, or Cu with nearly equal probability. The possible combinations of cloud types vertically are even more complicated when three-layer clouds are present (Figure 9d). In the tropics (red), while the upper layer is most likely Ci or As and the middle layer is mostly Ci or Ac, the lower layer can be any cloud type with only 15% of them being DC. In midlatitudes (yellow), however, MODIS HghThk clouds are infrequently (<6%) identified as DC in C-C. Clearly, caution is needed for cloud-type based analysis utilizing MODIS cloud regimes when multilayer clouds are present.

4. Summary and Discussion

Simultaneous cloud observations from both the CloudSat radar and CALIPSO lidar (C-C) provide accurate cloud frequency profiling, including clear sky and coexisting vertical layers across a variety of cloud types. We collocated MODIS daytime cloud observations of 1 km resolution to the C-C 2B-CLDCLASS-LIDAR product during 2007–2010 to establish connections of cloud observations between the passive imager and active profiling sensors. C-C vertical cloud frequency profiles are then used to validate MODIS cloud mask of confidently clear (Clr), probably clear (P.Clr), probably cloudy (P.Cldy), and confidently cloudy (Cldy). The MODIS multilayer flag was also evaluated with C-C cloud layers that are taken as a reference for true overlapping clouds in the atmosphere. Moreover, in Cldy single-layer cases we provide a cross-reference between MODIS cloud regimes following the CTP-τ definitions and C-C cloud types classified from a rule-based and fuzzy-logic-based classifiers combining many cloud properties such as base/top heights, horizontal extent, thermodynamic phase, spatial homogeneity, and the presence or absence of precipitation.

We confirm previous findings that the radiative cloud tops derived from MODIS generally agree with, but are slightly lower than, the physical cloud top in C-C (Figure 2). Overall, MODIS reports 30/58.7% confidently clear/cloudy sky, while C-C reports 27.1/72.9% due to its better sensitivity of cloud hydrometeors from combined cloud profile radar and lidar observations. C-C and MODIS generally agree in 77.8% of total observations, with 20.9% for both Clr and 56.9% for both Cldy conditions. Disagreement is found in 10.9% of strictly clear or cloudy scenes: 9.1% of observations are found Clr in MODIS but Cldy in C-C, indicating at least this percentage of clouds missed by MODIS; 1.8% of observations showing Cldy in MODIS but Clr in C-C is likely aerosol/dust or surface snow layers misidentified by MODIS.

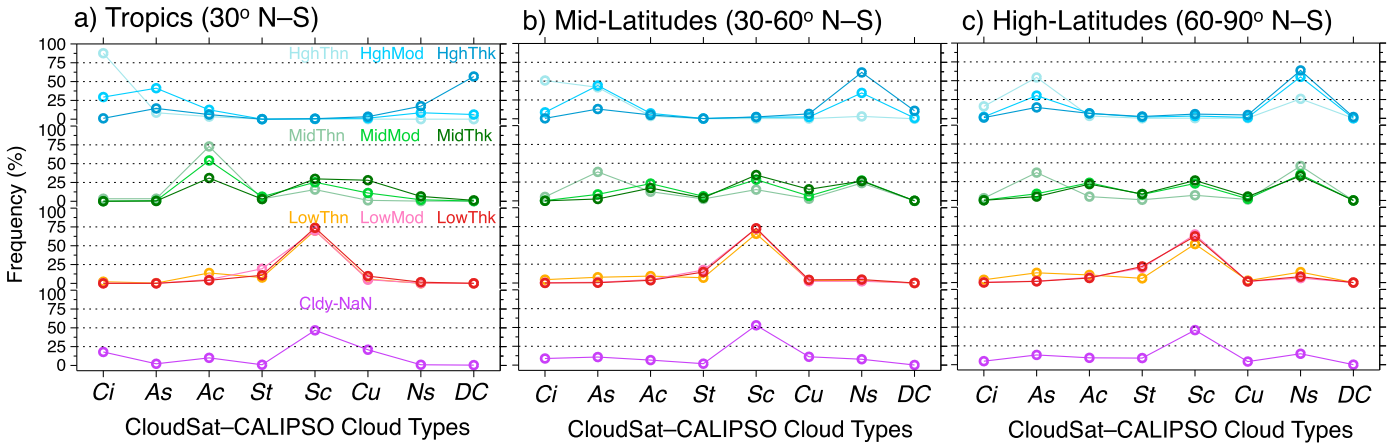

Figure 8. In single-layer cases, histograms of CloudSat-CALIPSO (C-C) cloud types for different MODIS cloud regimes in (a) the tropics, (b) the midlatitudes, and (c) the high latitudes in 2007–2010. Each line is normalized so that fractions of all CloudSat-CALIPSO cloud types sum to 100%.

Table 3. The Percentages Plotted in Figure 8[a]

	C-C								
MODIS	Ci	As	Ac	St	Sc	Cu	Ns	DC	Total (%)
Tropics (30°N–S)									
LowThn	2	0	14	8	70	6	0	0	100
LowMod	0	0	5	20	70	5	0	0	100
LowThnk	0	0	4	11	74	10	1	0	100
MidThn	3	4	73	3	16	1	0	0	100
MidMod	0	1	54	6	26	11	2	0	100
MidThk	0	0	31	3	30	28	7	1	100
HghThn	88	9	3	0	0	0	0	0	100
HghMod	30	41	12	0	1	1	9	6	100
HghThk	1	15	6	0	1	2	17	58	100
Cldy-NaN	18	2	10	1	47	21	1	0	100
Midlatitudes (30–60°N–S)									
LowThn	5	8	9	7	65	3	3	0	100
LowMod	1	1	5	17	72	2	2	0	100
LowThnk	0	0	4	15	73	4	4	0	100
MidThn	5	38	12	3	15	3	24	0	100
MidMod	0	9	23	6	28	7	27	0	100
MidThk	0	3	17	4	35	15	26	0	100
HghThn	51	42	4	0	0	0	3	0	100
HghMod	9	44	7	0	2	2	35	1	100
HghThk	1	13	5	0	2	7	61	11	100
Cldy-NaN	9	10	7	2	53	11	8	0	100
High Latitudes (60–90°N–S)									
LowThn	4	13	10	6	51	2	14	0	100
LowMod	0	2	7	20	64	1	6	0	100
LowThnk	0	2	6	21	61	2	8	0	100
MidThn	3	37	5	1	7	1	46	0	100
MidMod	0	9	24	8	23	2	34	0	100
MidThk	0	5	22	9	27	5	32	0	100
HghThn	16	54	4	0	0	0	26	0	100
HghMod	2	30	7	2	3	1	55	0	100
HghThk	1	15	7	2	6	4	63	2	100
Cldy-NaN	5	13	9	9	46	4	14	0	100

[a]This table quantifies the relations between MODIS cloud regimes and CloudSat-CALIPSO cloud classifications when single-layer cloud was observed by the CloudSat-CALIPSO.

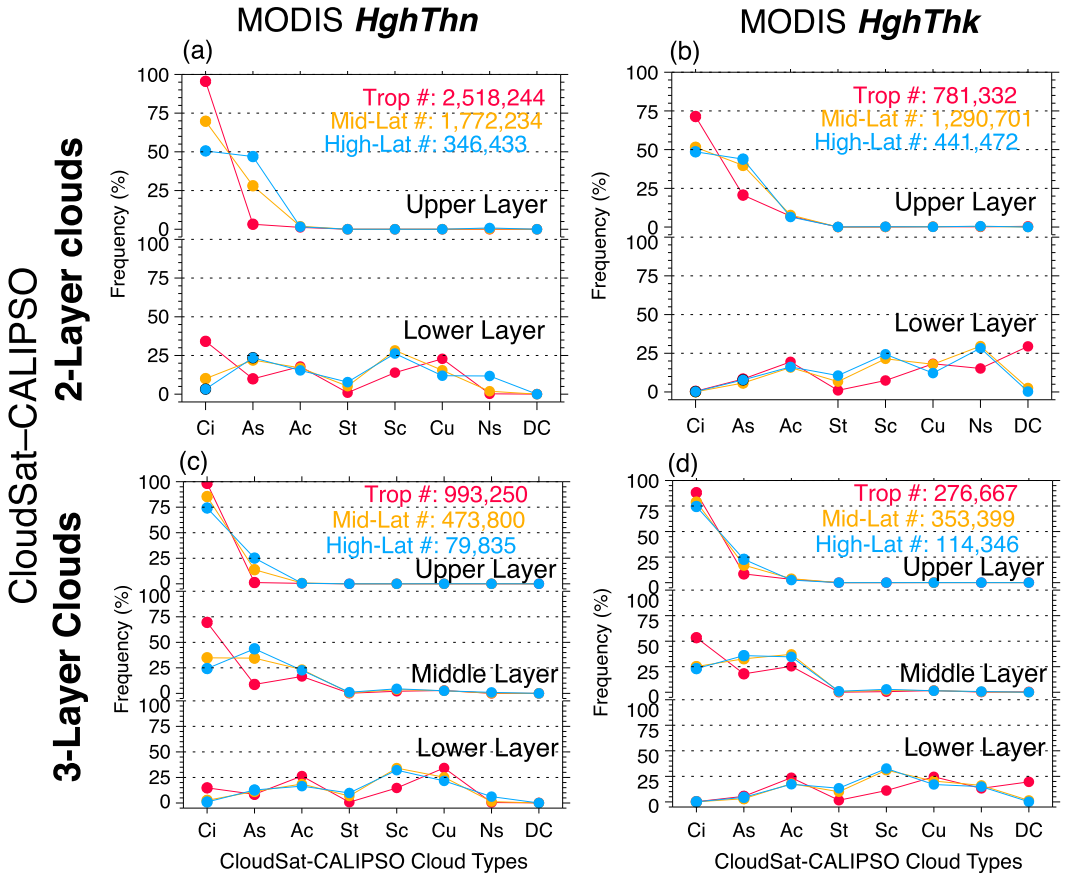

Figure 9. Under two- (a, b) and three-layer (c, d) cloudy conditions, histograms of CloudSat-CALIPSO (C-C) cloud types at each layer when MODIS identifies high-thin (HghThn, first column) and high-thick (HghThk, second column) clouds over the tropics (30°N–S, red), the midlatitudes (30–60°N–S, orange), and the high latitudes (60–90°N–S, blue) in 2007–2010. Each line is normalized so that fractions of all C-C cloud types sum to 100%.

In terms of single-layer and multilayer identification, MODIS only agrees with C-C for 25.4% of total observations, of which 17.7% are for single-layer cloud and 7.7% are for multilayer cloud. This is due to limitations of MODIS passive sensing of the whole vertical column that enables only identifying scenes of thin ice cloud on top of thicker water cloud in lower level [*Chang and Li*, 2005a, 2005b; *Wind et al*., 2010]. In contrast, C-C profiling is more capable of detecting multiple layers of clouds regardless cloud phase and cloud separation in the vertical (even two thin layers of cirrus on top of each other). Of the global observations during 2007–2010, MODIS reports 26.7% being single layer and 14.0% being multilayer, while C-C reports 47.4% and 25.5%, respectively. This C-C multilayer rate of 25.5% includes 19.1%, 5.2%, 1.0%, and 0.2% being two, three, four, and five layers, respectively.

Unlike the definitions of clear/cloudy conditions or single-layer/multilayer clouds that are consistent across different platforms, the definition applied to MODIS and C-C for obtaining cloud classifications are necessarily different because of the vastly different observing techniques. MODIS cloud regimes are simply defined by bins in CTP-τ histograms whereas C-C cloud types are based on several morphological cloud characteristics such as cloud base/top heights, thermodynamic phase, spatial homogeneity, horizontal extent, and the presence or absence of precipitation. Thus, studies using C-C cloud types [e.g., *Jiang et al*., 2011; *Li et al*., 2015] are not necessarily comparable to those using MODIS cloud regimes [e.g., *Wang et al*., 2015]. We cross-referenced the two sets of cloud classifications for single-layer clouds. We found that in the tropics, ~90% of tropical MODIS high and optically thin clouds (HghThn) are identified as cirrus (Ci) in C-C and ~60% of MODIS high and optically thick (HghThk) clouds are identified as deep convective (DC). MODIS low-level clouds, regardless of thickness and regions, are consistently (~70%) classified as stratocumulus (Sc) in C-C. MODIS middle-level clouds, however, have no clear relationships to C-C cloud types. In cases of

multilayer clouds, simple MODIS cloud regimes correspond to more complicated combinations of C-C multilayer cloud types. For example, the combination of optically thin Ci on top of low- and middle-level clouds is frequently observed as HghThk clouds in MODIS. For multilayer clouds, caution is needed when applying retrievals from passive sensors to define cloud types.

Our results address the fundamental differences of passive and active remote sensing of clouds. Cloud vertical structure from active sensors is necessary for the interpretation of MODIS images. The comparisons should be taken into context when observing clouds from either perspective. While the active systems are more sensitive to clouds, we emphasize that we do not suggest that one classification system is superior to another but provide a cross-reference of their relationships toward the goal of improved quantification of different cloud types.

Acknowledgments

We thank Bryan A. Baum from the University of Wisconsin-Madison, Zhien Wang from the University of Wyoming, Tianle Yuan from NASA Goddard Space Flight Center, and Fu-Lung Chang from the NASA Langley Research Center for many helpful and inspiring discussions. We also thank Mathias Schreier at JPL for providing help downloading MODIS C6 data from GSFC LAADS WEB (ftp://lads-web.nascom.nasa.gov/allData/6/). CloudSat data were obtained through the CloudSat Data Processing Center (http://www.cloudsat.cira.colostate.edu/). The research described in this paper was carried out at the Jet Propulsion Laboratory, California Institute of Technology, under a contract with the National Aeronautics and Space Administration. This work is supported by NASA Making Earth System data records for Use in Research Environments (MEaSUREs, NNH12ZDA001-MEASURES) and NASA Modeling, Analysis, and Prediction (MAP, NNH12ZDA001-MAP) projects. © 2016. California Institute of Technology. Government sponsorship acknowledged.

References

Baum, B. A., and B. A. Wielicki (1994), Cirrus cloud retrieval using infrared sounding data: Multilevel cloud errors, *J. Appl. Meteorol.*, *33*, 107–117, doi:10.1175/1520-0450(1994)033<0107:CCRUIS>2.0.CO;2.

Baum, B. A., P. W. Menzel, R. A. Frey, D. C. Tobin, R. E. Holz, S. A. Ackerman, A. K. Heidinger, and P. Yang (2012), MODIS cloud-top property refinements for Collection 6, *J. Appl. Meteorol. Climatol.*, *51*, 1145–1163, doi:10.1175/JAMC-D-11-0203.1.

Bromwich, D. H., et al. (2012), Tropospheric clouds in Antarctica, *Rev. Geophys.*, *50*, RG1004, doi:10.1029/2011RG000363.

Chang, F.-L., and Z. Li (2005a), A new method for detection of cirrus-overlapping-water clouds and determination of their optical properties, *J. Atmos. Sci.*, *62*, 3993–4009.

Chang, F.-L., and Z. Li (2005b), A near-global climatology of single-layer and overlapped clouds and their optical properties retrieved from Terra/MODIS data using a new algorithm, *J. Clim.*, *18*, 4752–4771.

Davis, S. M., L. M. Avallone, B. H. Kahn, K. G. Meyer, and D. Baumgardner (2009), Comparison of airborne in situ measurements and Moderate Resolution Imaging Spectroradiometer (MODIS) retrievals of cirrus cloud optical and microphysical properties during the Midlatitude Cirrus Experiment (MidCiX), *J. Geophys. Res.*, *114*, D02203, doi:10.1029/2008JD010284.

Dessler, A. E., and P. Yang (2003), The distribution of tropical thin cirrus clouds inferred from Terra MODIS data, *J. Clim.*, *16*, 1241–1247, doi:10.1175/1520-0442(2003)16<1241:TDOTTC>2.0.CO;2.

Frey, R., S. Ackerman, Y. Liu, K. Strabala, H. Zhang, J. Key, and X. Wang (2008), Cloud detection with MODIS. Part I: Improvements in the MODIS cloud mask for Collection 5, *J. Atmos. Oceanic Technol.*, *25*, 1057–1072, doi:10.1175/2008JTECHA1052.1.

Holz, R. E., S. A. Ackerman, F. W. Nagle, R. Frey, S. Dutcher, R. E. Kuehn, M. A. Vaughan, and B. Baum (2008), Global Moderate Resolution Imaging Spectroradiometer (MODIS) cloud detection and height evaluation using CALIOP, *J. Geophys. Res.*, *113*, D00A19, doi:10.1029/2008JD009837.

Jiang, X., D. E. Waliser, J.-L. Li, and C. Woods (2011), Vertical structures of cloud water associated with the boreal summer intraseasonal oscillation based on CloudSat observations and ERA-Interim reanalysis, *Clim. Dyn.*, *36*, 2219–2232, doi:10.1007/s00382-010-0853-8.

Joiner, J., A. P. Vasilkov, P. K. Bhartia, G. Wind, S. Platnick, and W. P. Menzel (2010), Detection of multilayer and vertically extended clouds using A-Train sensors, *Atmos. Meas. Tech.*, *3*, 233–247.

Kahn, B. H., et al. (2008), Cloud type comparisons of AIRS, CloudSat, and CALIPSO cloud height and amount, *Atmos. Chem. Phys.*, *8*, 1231–1248, doi:10.5194/acp-8-1231-2008.

King, M. D., Y. J. Kaufman, W. P. Menzel, and D. Tanre (1992), Remote sensing of cloud, aerosol and water vapor properties from the moderate resolution imaging spectrometer (MODIS), *IEEE Trans. Geosci. Remote Sens.*, *30*, 2–27.

King, M. D., W. P. Menzel, Y. J. Kaufman, D. Tanré, B. C. Gao, S. Platnick, S. A. Ackerman, L. A. Remer, R. Pincus, and P. A. Hubanks (2003), Cloud, aerosol and water vapor properties from MODIS, *IEEE Trans. Geosci. Remote Sens.*, *41*, 442–458.

King, M. D., S. Platnick, W. P. Menzel, S. A. Ackerman, and P. A. Hubanks (2013), Spatial and temporal distribution of clouds observed by MODIS onboard the Terra and Aqua satellites, *IEEE Trans. Geosci. Remote Sens.*, *51*, 3826–3852.

Klein, S. A., D. L. Hartmann, and J. R. Norris (1995), On the relationships among low-cloud structure, sea surface temperature and atmospheric circulation in the summertime northeast Pacific, *J. Clim.*, *8*, 1140–1155.

Li, J., J. Huang, K. Stamnes, T. Wang, Q. Lv, and H. Jin (2015), A global survey of cloud overlap based on CALIPSO and CloudSat measurements, *Atmos. Chem. Phys.*, *15*(1), 519–536.

Mace, G. G., Q. Zhang, M. Vaughan, R. Marchand, G. Stephens, C. Trepte, and D. Winker (2009), A description of hydrometeor layer occurrence statistics derived from the first year of merged Cloudsat and CALIPSO data, *J. Geophys. Res.*, *114*, D00A26, doi:10.1029/2007JD009755.

Mace, G. G., S. Houser, S. Benson, S. A. Klein, and Q. Min (2011), Critical evaluation of the ISCCP simulator using ground-based remote sensing data, *J. Clim.*, *24*, 1598–1612.

Marchand, R., G. G. Mace, T. Ackerman, and G. Stephens (2008), Hydrometeor detection using *CloudSat*—An Earth-orbiting 94-GHz cloud radar, *J. Atmos. Oceanic Technol.*, *25*, 519–533.

Marchand, R., T. Ackerman, M. Smythe, and W. B. Rossow (2010), A review of cloud top height and optical depth histograms from MISR, ISCCP and MODIS, *J. Geophys. Res.*, *115*, D16206, doi:10.1029/2009JD013422.

Menzel, W. P., R. A. Frey, H. Zhang, D. P. Wylie, C. C. Moeller, R. A. Holz, B. Maddux, B. A. Baum, K. I. Strabala, and L. E. Gumley (2008), MODIS global cloud-top pressure and amount estimation: Algorithm description and results, *J. Appl. Meteorol. Clim.*, *47*, 1175–1198.

Menzel, W. P., R. A. Frey, and B. A. Baum (2015), Cloud top properties and cloud phase algorithm theoretical basis document, May 2015, available at http://modis-atmos.gsfc.nasa.gov/_docs/MOD06-ATBD_2015_05_01.pdf

Partain, P. (2007), *CloudSat Project: Cloudsat ECMWF-AUX Auxiliary Data Process Description and Interface Control Document*, 11 pp., Colo. State Univ., Fort Collins, Colo.

Pavolonis, M. J., and A. K. Heidinger (2004), Daytime cloud overlap detection from AVHRR and VIIRS, *J. Appl. Meteorol.*, *43*, 762–778.

Pincus, R., S. Platnick, S. A. Ackerman, R. S. Hemler, and R. J. P. Hofmann (2012), Reconciling simulated and observed views of clouds: MODIS, ISCCP, and the limits of instrument simulators, *J. Clim.*, doi:10.1175/JCLI-D-11-00267.1.

Platnick, S., M. D. King, S. A. Ackerman, W. P. Menzel, B. A. Baum, J. C. Riédi, and R. A. Frey (2003), The MODIS cloud products: Algorithms and examples from Terra, *IEEE Trans. Geosci. Remote Sens.*, *41*, 459–473.

Platnick, S., et al. (2013), MODIS cloud optical properties: User guide for the Collection 6 level-2 MOD06/MYD06 product and associated level-3 datasets, MODIS MOD06 User Guide.

Platnick, S., Ackerman, S., King, M., K. G. Meyer, W. P. Menzel, R. E. Holz, B. A. Baum, and P. Yang, (2015), MODIS Atmosphere L2 Cloud: Product (06_L2), NASA MODIS Adaptive Processing System, Goddard Space Flight Center, doi:10.5067/MODIS/MYD06_L2.006.

Rossow, W. B., and R. A. Schiffer (1999), Advances in understanding clouds from ISCCP, *Bull. Am. Meteorol. Soc.*, *80*, 2261–2287, doi:10.1175/1520-0477(1999)080<2261:AIUCFI>2.0.CO;2.

Sassen, K., and G. G. Mace (2002), Ground based remote sensing of cirrus clouds, in *Cirrus*, edited by D. Lynch et al., pp. 168–195, Oxford Univ. Press, New York.

Stephens, G. L., et al. (2002), The CloudSat mission and the A-Train: A new dimension of space-based observations of clouds and precipitation, *Bull. Am. Meteorol. Soc.*, *83*, 1771–1790.

Suzuki, K., T. Y. Nakajima, and G. L. Stephens (2010), Particle growth and drop collection efficiency of warm clouds as inferred from joint CloudSat and MODIS observations, *J. Atmos. Sci.*, *67*(9), 3019–3032, doi:10.1175/2010JAS3463.1.

Vaughan, M. A., S. A. Young, D. M. Winker, K. A. Powell, A. H. Omar, Z. Liu, Y. Hu, and C. A. Hostetler (2004), Fully automated analysis of space-based lidar data: An overview of the CALIPSO retrieval algorithms and data products, *Remote Sens.*, *5575*, 16–30, doi:10.1117/12.572024.

Wang, T., and A. E. Dessler (2012), Analysis of cirrus in the tropical tropopause layer from CALIPSO and MLS data: A water perspective, *J. Geophys. Res.*, *117*, D04211, doi:10.1029/2011JD016442.

Wang, T., S. Wong, and E. J. Fetzer (2015), Cloud regime evolution in the Indian monsoon intraseasonal oscillation: Connection to large-scale dynamical conditions and the atmospheric water budget, *Geophys. Res. Lett.*, *42*, 9465–9472, doi:10.1002/2015GL066353.

Wang, Z., and K. Sassen (2001), Cloud type and macrophysical property retrieval using multiple remote sensors, *J. Appl. Meteorol.*, *40*, 1665–1682.

Wang, Z., et al. (2013), *CloudSat Project: Level 2 Combined Radar and Lidar Cloud Scenario Classification Product Process Description and Interface Control Document*, 61 pp., California Institute of Technology, Calif.

Wind, G., S. Platnick, M. D. King, P. A. Hubanks, B. A. Baum, M. J. Pavolonis, A. K. Heidinger, P. Yang, and D. P. Kratz (2010), Multilayer cloud detection with MODIS near-infrared water vapour absorption band, *J. Appl. Meteorol. Climatol.*, *49*, 2315–2333, doi:10.1175/2010JAMC2364.1.

Winker, D. M., W. H. Hunt, and M. J. McGill (2007), Initial performance assessment of CALIOP, *Geophys. Res. Lett.*, *34*, L19803, doi:10.1029/2007GL030135.

Wong, S., E. J. Fetzer, M. Schreier, G. Manipon, E. F. Fishbein, B. H. Kahn, Q. Yue, and F. W. Irion (2015), Cloud-induced uncertainties in AIRS and ECMWF temperature and specific humidity, *J. Geophys. Res. Atmos.*, *120*, 1880–1901, doi:10.1002/2014JD022440.

Yuan, T., and L. Oreopoulos (2013), On the global character of overlap between low and high clouds, *Geophys. Res. Lett.*, *40*, 5320–5326, doi:10.1002/grl.50871.